Intense, Narrow Atomic-Clock Resonances

Y.-Y. Jau,[1] A. B. Post,[1] N. N. Kuzma,[1] A. M. Braun,[2] M.V. Romalis,[1] and W. Happer[1]
[1]*Department of Physics, Princeton University, Princeton, New Jersey 08544, USA*
[2]*Sarnoff Corporation, Princeton, New Jersey 08543, USA*
(Received 14 August 2003; published 18 March 2004)

We present experimental and theoretical results showing that magnetic resonance transitions from the "end" sublevels of maximum or minimum spin in alkali-metal vapors are a promising alternative to the conventional 0-0 transition for small-size gas-cell atomic clocks. For these "end resonances," collisional spin-exchange broadening, which often dominates the linewidth of the 0-0 resonance, decreases with increasing spin polarization and vanishes for 100% polarization. The end resonances also have much stronger signals than the 0-0 resonance, and are readily detectable in cells with high buffer-gas pressure.

DOI: 10.1103/PhysRevLett.92.110801 PACS numbers: 06.30.Ft, 32.10.Fn, 32.80.Bx, 52.70.Gw

Atomic clocks based on spin-polarized alkali-metal atoms [1] have been traditionally built by locking a microwave harmonic of a quartz crystal frequency to the Bohr frequency of a 0-0 hyperfine resonance. The experiments reported here demonstrate that the "end resonances" of alkali-metal vapors have important advantages over the 0-0 resonance in miniature gas-cell atomic clocks [2–5].

The hyperfine sublevels of the ground state of a typical alkali-metal atom are sketched in Fig. 1. The two hyperfine multiplets have the total spin quantum numbers $f = I + 1/2 = a$ and $f = I - 1/2 = b$, where I is the spin quantum number of the nucleus. For magnetic fields typically used in atomic clocks, f remains very nearly a good quantum number. We denote the energy eigenstates by $|f, m\rangle$, where m is the projection of the total spin along the magnetic field B.

The shift of the 0-0 resonance frequency by the magnetic field is small and quadratic in B, while the end resonances have a much larger linear shift with B. The 0-0 resonance has an advantage of being weakly field dependent; however, it has three serious disadvantages.

Population dilution.—Only a small fraction of the atoms can contribute to the 0-0 resonance intensity, since most of the atoms are in states with $m \neq 0$. For example, in ^{133}Cs ($I = 7/2$) a traditional pumping scheme with monochromatic light at low buffer-gas pressure can remove the atoms from the upper multiplet and distribute them approximately uniformly among the seven sublevels of the lower multiplet, so only $1/7$ of the atoms participate in the resonance. One can achieve higher efficiencies using multistep preparation techniques [6], but they are not easily applicable to continuous-mode gas-cell clocks.

Spin-exchange broadening.—Spin exchange [7,8], which is often the dominant relaxation process at high alkali-metal densities, causes the 0-0 coherence in a weakly polarized vapor to damp at a rate $\Gamma_{ex}(3/4 - 1/g)$, where Γ_{ex} is the spin-exchange rate and $g = 2(2I + 1)$ is the total number of ground-state sublevels.

Poor pumping efficiency at high gas pressures.—Buffer gases are normally used to limit the rate at which pumped atoms diffuse to and relax at the cell walls. Buffer gases also broaden the optical absorption lines. At gas pressures exceeding a few hundred torr, collisional broadening causes the hyperfine components of the optical absorption lines to overlap, diminishing the efficiency of pumping from one hyperfine multiplet to the other.

The second and third disadvantages are particularly serious if one tries to reduce the size of a gas-cell atomic clock. The frequency stability of the clock is of order $\delta\nu \sim \Delta\nu/\mathrm{SNR}$, where $\Delta\nu$ is the full width at half maximum of the resonance line and SNR is the signal-to-noise ratio. In miniaturized cells, the alkali vapor density must be increased to maintain the absorption signal from the pumping light, and the buffer-gas density must be increased to hinder vapor diffusion to the cell walls.

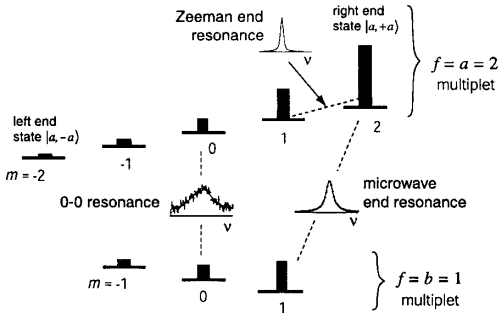

FIG. 1. Energy sublevels of the ground state of an alkali-metal atom in a small magnetic field (not to scale). The nuclear spin quantum number in this illustration is $I = 3/2$. The three insets show examples of observed resonance curves (signal intensity vs frequency) for the 0-0 resonance, a microwave end resonance, and a Zeeman end resonance, all in ^{87}Rb at 140 °C. The corresponding linewidths are $\Delta\nu = 8.6$, 2.6, and 1.1 kHz. Spin exchange causes the 0-0 resonance to be broader and have a hundred times poorer signal-to-noise ratio (SNR) than the end resonances.

Spin-exchange and buffer-gas collisions broaden the linewidth $\Delta\nu$. The collisions also decrease the SNR, since they tend to equalize the populations of the initial and final states of the transition, and they decrease the pumping efficiency, as outlined above. So the frequency stability of miniature clocks operating on the 0-0 resonance is diminished because of both larger $\Delta\nu$ and smaller SNR.

Our recent experiments indicate that the end resonances, involving transitions from one of the two "end states" $|a, +a\rangle$ or $|a, -a\rangle$ of Fig. 1, can be much less affected [9] by the disadvantages mentioned above. By using left- or right-circularly polarized $D1$ light, nearly all of the atoms can be pumped into one or the other end state. This eliminates the population dilution problem in a very simple way and greatly increases the SNR of the resonance. Pumping with circularly polarized $D1$ light works very well at high buffer-gas pressures, despite the overlap of the hyperfine components of the absorption lines caused by pressure broadening. Finally, when nearly all the atoms are in one of the end states, the spin-exchange broadening of the resonance nearly vanishes. This is because spin-exchange collisions conserve the total spin angular momentum—if both colliding atoms start in the same end state, spin-exchange transitions to all other states are forbidden.

To cope with the relatively large, linear magnetic field dependence of the end resonance frequencies, one can actively control both the magnetic field B and local oscillator frequency, using simultaneous feedback signals from the microwave and Zeeman end resonances. The frequencies of these two resonances can be generated as harmonics or subharmonics of the same local oscillator frequency, so that their ratio is a fixed integer. Analysis shows that the Allan deviation of the clock frequency ν should be proportional to $\delta\nu/\nu = \Delta\nu_m(\nu\mathrm{SNR}_m)^{-1} + 2I\Delta\nu_Z(\nu\mathrm{SNR}_Z)^{-1}$. The Zeeman linewidth $\Delta\nu_Z$ is typically smaller than the microwave linewidth $\Delta\nu_m$ by at least a factor of $2I$ (see Fig. 4 below). The signal-to-noise ratios SNR_m and SNR_Z are about the same. So having to lock the magnetic field (in addition to locking the local oscillator frequency) approximately doubles the Allan variance of a clock, which is a small penalty compared to the advantages of a narrower $\Delta\nu$ and a much higher SNR, demonstrated for the end resonances in this Letter.

For alkali-metal atoms, pumped by circularly polarized light propagating along the magnetic field in a buffer-gas cell, there are the following major contributions to the resonance linewidth: (1) Spin-exchange collisions [7,8] with other alkali-metal atoms at a rate Γ_{ex}. (2) Collisions with buffer-gas atoms. The gas-induced spin relaxation is characterized by an S-damping rate Γ_{sd}, which parametrizes damping from the spin-rotation interaction [10,11], and a Carver rate Γ_{C}, which parametrizes [1,12,13] homogeneous damping due to the collisional modulation of the hyperfine coupling. (3) Diffusion to the cell walls, which we parametrize with the damping rate Γ_{d} of the slowest spatial diffusion mode. (4) Optical pumping, parametrized by Γ_{op}, the absorption rate of pumping photons by unpolarized atoms, and by the mean photon spin s ($s = \pm 1$ for circularly polarized light). We assume the cells contain a sufficient amount of quenching N_2 gas that the spin relaxation due to radiation trapping is negligible [14,15]. (5) Microwave power broadening. (6) Inhomogeneities in the static magnetic field, which we denote by $\Gamma_{\nabla B}$. (7) Broadening due to temperature inhomogeneities, which we denote by $\Gamma_{\nabla T}$. This broadening is a consequence of the pressure shift [16,17] of the hyperfine frequency of alkali-metal atoms in buffer gases. The gas density is lower in hotter parts of the cell, so the density-induced frequency shift is smaller. The $\Gamma_{\nabla T}$ broadening of the microwave linewidths equals the homogeneous broadening [13] in the gases He, N_2, and Ar if temperature variations across the cells are approximately 0.6, 0.8, and 3.7 °C, respectively. Since $\Gamma_{\nabla T}$ is proportional to gas pressure, it can easily be mistaken for homogeneous broadening.

In addition to the buffer-gas shift, the hyperfine reference frequency can also be affected by the light shift [18,19] and the spin-exchange frequency shift [6,7]. These shifts can be suppressed by an appropriate choice of laser frequency and a high spin polarization.

The combined effects of spin-exchange collisions, collisions with the buffer-gas atoms, and optical pumping at high pressure produce an exact spin-temperature distribution of alkali populations [11], such that the probability of finding an atom in the state $|i\rangle = |f_i, m_i\rangle$ is $\rho_{ii} = e^{\beta m_i}/Z$, with the partition function $Z = \sum_i e^{\beta m_i}$. The electron spin polarization $P = 2\langle S_z\rangle$, twice the mean electron spin $\langle S_z\rangle$, is related to the spin-temperature parameter β by $P = \tanh(\beta/2) = s\Gamma_{\mathrm{op}}/(\Gamma_{\mathrm{op}} + \Gamma_{\mathrm{sd}})$. Neither spin-exchange nor the Carver rate affects the equilibrium polarization P.

Diffusion to the walls prevents the population distribution from being exactly described by a spin temperature. But if the diffusion contribution is not too large, as was the case in our experiments, a spin-temperature distribution is still a good approximation, and $P = s\Gamma_{\mathrm{op}}/(\Gamma_{\mathrm{op}} + \Gamma^*_{\mathrm{sd}})$, where $\Gamma^*_{\mathrm{sd}} = \Gamma_{\mathrm{sd}} + (1 + \epsilon)\Gamma_d$. This is a polynomial equation in P, since the paramagnetic coefficient $\epsilon = \langle I_z\rangle/\langle S_z\rangle$, the ratio of the mean nuclear spin $\langle I_z\rangle$ to $\langle S_z\rangle$, is a rational function of P [11].

In the limit of vanishing microwave or radio-frequency power, and for spin populations well described by a spin temperature, the main contributions [9,11] to the damping rate for coherence between sublevels $|a, \overline{m} \pm 1/2\rangle$ and $|b, \overline{m} \mp 1/2\rangle$ are given by

$$\Gamma = (\Gamma_{\mathrm{ex}} + \Gamma_{\mathrm{sd}} + \Gamma_{\mathrm{op}})\left(\frac{3}{4} + \frac{4\overline{m}^2 - 1}{4[I]^2}\right) \mp \frac{P\Gamma_{\mathrm{ex}} + s\Gamma_{\mathrm{op}}}{2[I]} + \Gamma_{\mathrm{C}}\frac{\eta_I^2[I]^2}{8} - \Gamma_{\mathrm{ex}}Q_{\overline{m}}\frac{([I] \pm 2\overline{m})^2 - 1}{4[I]^2} + \Gamma_{\mathrm{d}} + \Gamma_{\mathrm{in}}. \quad (1)$$

The contribution of the inhomogeneous damping mechanisms is $\Gamma_{\mathrm{in}} = \Gamma_{\nabla T} + \Gamma_{\nabla B}$. The Carver rate Γ_{C} [13] is the

same for all isotopes of a given alkali metal, and can be determined experimentally [13]. The isotope coefficient is $\eta_I = \mu_I/(2I\mu_N)$, where μ_I and μ_N are the nuclear magnetic moment and nuclear magneton. We denote the probability to find the nucleus with an azimuthal quantum number $\overline{m}$ by $Q_{\overline{m}} = e^{\beta\overline{m}}/Z_I$, where $Z_I = \sum_{m_I} e^{\beta m_I}$.

Similarly, the damping rate for a Zeeman resonance between sublevels $|f, \overline{m} \pm 1/2\rangle$ and $|f, \overline{m} \mp 1/2\rangle$ is given by

$$\Gamma = (\Gamma_{ex} + \Gamma_{sd} + \Gamma_{op})\left[\frac{3}{4} - \frac{4\overline{m}^2 - 1}{4[I]^2}\right] - \frac{(P\Gamma_{ex} + s\Gamma_{op})\overline{m}}{2(f-I)[I]} - \Gamma_{ex} Q_{\overline{m}} \frac{[f]^2 - 4\overline{m}^2}{4[I]^2} + \Gamma_d + \Gamma_{in}. \quad (2)$$

It follows from Eqs. (1) and (2) that the contribution of spin exchange to microwave and Zeeman resonances $|a, \pm a\rangle \leftrightarrow |b, \pm b\rangle$ and $|a, \pm a\rangle \leftrightarrow |a, \pm b\rangle$ vanishes as $P \rightarrow \pm 1$. The suppression of spin-exchange broadening as $P \rightarrow \pm 1$ for Zeeman end resonances, as described by Eq. (2), has already been observed [20].

We have experimentally demonstrated the high signal-to-noise ratio and the suppression of spin-exchange line broadening for microwave end resonances with the apparatus shown in Fig. 2. Isotopically enriched Rb metal (99.1% ^{87}Rb) was distilled into four Pyrex-glass cells, with flat compartments (1 mm interwall spacing) and 3.6 cm^3 spherical ballast compartments. The cells were filled with N_2 gas, at number densities $[N_2] = 0.96$, 1.9, 2.8, and 3.7 amg (1 amg $= 2.687 \times 10^{19}$ cm^{-3}), as determined by the pressure and temperature of the gas during sealoff with a flame. The cells were mounted in a temperature-controlled, air-heated nonmagnetic oven. Three sets of Helmholtz coils were used to obtain a small static magnetic field B, parallel to the pumping light and normal to the flat cell walls. The static field was 4.6 G, so the microwave and the Zeeman frequencies were about 6.84 GHz and 3.2 MHz. To drive the magnetic resonances, microwaves (from a horn antenna located 6 cm away) or an rf field (from a small coil) were used. The Rabi frequency, $\omega_r \approx 2\pi \times 100$ Hz, made a negligible contribution to the measured linewidth. The light from an external-cavity diode laser, operating at the 795-nm Rb $D1$ line, was circularly polarized and the beam intensity was adjusted from 0.1 to 20 mW cm^{-2}. The diameter of the beam at the cell was about 3 mm, so the volume of the irradiated vapor was $\sim$7 mm^3. The intensities of both the transmitted and the incident lights were continuously monitored using photodiodes, and fed into an analog divider circuit, to eliminate some of the intensity fluctuations. The resulting signal was amplified, digitized, and recorded. To measure the damping rate predicted by Eq. (1), two different experimental methods were used. In the traditional method, the resonances were recorded by slowly scanning the microwave frequency, modulating the microwaves incident on the cell with a 50 Hz square wave, and detecting the resulting modulation of the transmitted light with a lock-in amplifier. The resonance curve, broadened by the microwave power P_μ, had a width $\Delta\nu = (\Gamma + \tau\omega_r^2)/\pi$, where τ is a constant. To extract Γ it was necessary to record data for several values of P_μ, and to extrapolate the resulting $\Delta\nu$ to zero P_μ. A faster measurement method was to observe a damped transient oscillation of the transmitted light intensity, when the microwave or rf power was suddenly turned on with a detuning $|\omega - \omega_0| \gg \omega_r$. The complex frequency of the transient is $\tilde{\Omega} = \sqrt{(\omega - \omega_0)^2 + \omega_r^2} + i\Gamma$, so a Fourier transform of the transient is a Lorentzian curve with a width Γ. For typical detunings, $|\omega - \omega_0|/2\pi \gtrsim 5$ kHz, the signal was free from low-frequency noise. We verified that the values of Γ obtained by the two methods were consistent.

Figure 3 shows the dependence of the microwave end resonance linewidth on the pumping laser-light intensity

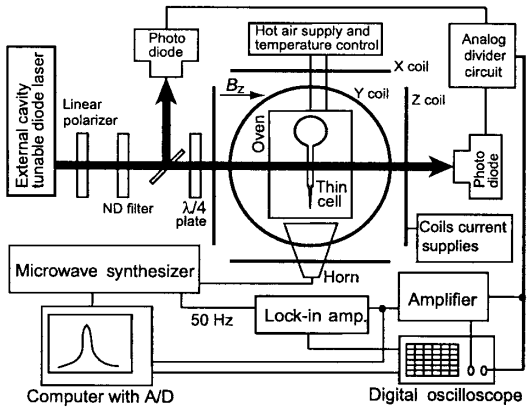

FIG. 2. The apparatus for magnetic resonance studies.

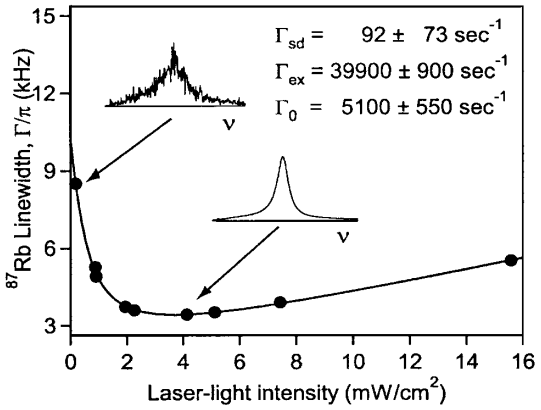

FIG. 3. The ^{87}Rb linewidth of a microwave end resonance measured as a function of laser-light intensity at 140 °C, $[N_2] = 0.96$ amg, using the frequency-scanning method. The solid curve is the fit of Γ/π from Eq. (1) to the experimental data, using a fixed estimate $\Gamma_d = 111$ s^{-1} [21]. The fitting parameters Γ_{sd} and Γ_{ex} are consistent with the measurement of Walter *et al.* [13]. Γ_0 is the sum of contributions from Γ_C and Γ_{in}. The insets show experimental resonance curves at the two light-intensity points indicated.

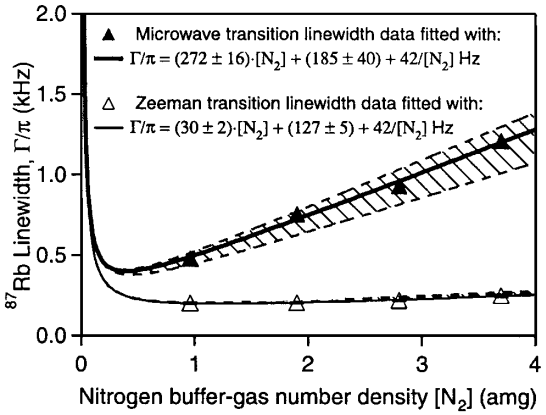

FIG. 4. Dependence of the microwave and Zeeman end resonance linewidths on the nitrogen buffer-gas density at 60 °C, obtained using the transient method. The $[N_2]$-independent baseline is due to Γ_{ex} and residual inhomogeneity $\Gamma_{\nabla B}$. The hatched areas bounded by dashed lines show the linewidth predictions for the two resonances, based on the data of Walter *et al.* [13]. Compared to the microwave resonance, the Zeeman linewidth shows much less broadening, since it is not affected by the Carver rate Γ_C.

at high alkali-metal density. At low light intensity the spin polarization P is close to zero and the linewidth is dominated by spin-exchange collisions. Increasing the laser intensity increases the spin polarization P and reduces the spin-exchange broadening. For sufficiently large laser power, the line *narrowing* due to a decreased spin-exchange contribution as $P \to 1$ is counterbalanced by the line *broadening* due to increased photon-scattering. From examination of Eq. (1) one can show that the minimum linewidth is given by $\Gamma/\pi = c\sqrt{\Gamma_{ex}\Gamma_{sd}^*} +$ const, where $c \approx 0.4$ depends weakly on P, I, etc.

Figure 4 shows the microwave and Zeeman linewidths as a function of N_2 buffer-gas pressure at low alkali-metal density and laser power. It demonstrates that the Carver rate Γ_C dominates the contribution of the buffer gas to the linewidth of the microwave end resonance, since Γ_C is the only parameter of Eq. (1) that does not contribute to the Zeeman linewidth of Eq. (2). The broadening parameters we used for nitrogen [13] to obtain the hatched areas of Fig. 4 are substantially smaller than those one can infer from the pioneering work of Vanier *et al.* [21]. It is possible that there were unrecognized contributions of temperature gradients in that work [22].

In conclusion, we have demonstrated, for the first time, that the microwave end resonances of highly spin-polarized alkali-metal vapors have exceptionally high signal-to-noise ratios (due to reduced population dilution) and narrower linewidths (due to suppression of spin exchange) than the 0-0 resonance. We have also shown that the broadening of the resonance lines by buffer gases is substantially smaller than the early measurements would lead one to expect.

For the future miniature gas-cell atomic clocks, it may be advantageous to eliminate the need for a microwave generator by exciting coherent population trapping (CPT) resonances [2,3,23,24] with light modulated at the Bohr frequency, or a subharmonic [4,5]. The CPT *end resonances* will still be free from spin-exchange broadening, given by Eq. (1).

We are grateful to M. Souza for cell design and to J. Vanier, D. Walter, and K. Gibble for discussions. This work was supported by the AFOSR and DARPA.

[1] J. Vanier and C. Audoin, *The Quantum Physics of Atomic Frequency Standards* (A. Hilger, Philadelphia, 1989).
[2] A. Godone, F. Levi, and J. Vanier, IEEE Trans. Instrum. Meas. **48**, 504 (1999).
[3] N. Cyr, M. Tetu, and M. Breton, IEEE Trans. Instrum. Meas. **42**, 640 (1993).
[4] J. Kitching, S. Knappe, and L. Hollberg, Appl. Phys. Lett. **81**, 553 (2002).
[5] J. Kitching, L. Hollberg, S. Knappe, and R. Wynands, Electron. Lett. **37**, 1449 (2001).
[6] C. Fertig and K. Gibble, Phys. Rev. Lett. **85**, 1622 (2000).
[7] L. C. Balling, F. M. Pipkin, and R. J. Hanson, Phys. Rev. **133**, A607 (1964).
[8] F. Grossetête, J. Phys. (Paris) **25**, 383 (1964).
[9] D. K. Walter and W. Happer, Laser Phys. **12**, 1182 (2002).
[10] R. A. Bernheim, J. Chem. Phys. **36**, 135 (1962).
[11] S. Appelt, A. B.-A. Baranga, C. J. Erickson, M. V. Romalis, A. R. Young, and W. Happer, Phys. Rev. A **58**, 1412 (1998).
[12] H. Margenau, P. Fontana, and L. Klein, Phys. Rev. **115**, 87 (1959).
[13] D. K. Walter, W. M. Griffith, and W. Happer, Phys. Rev. Lett. **88**, 093004 (2002).
[14] P. Davidovits and R. Novick, Proc. IEEE **54**, 155 (1966).
[15] D. Tupa and L. W. Anderson, Phys. Rev. A **36**, 2142 (1987).
[16] M. Arditi and T. R. Carver, Phys. Rev. **112**, 449 (1958).
[17] B. L. Bean and R. H. Lambert, Phys. Rev. A **12**, 1498 (1975).
[18] J. P. Barrat and C. Cohen-Tannoudji, J. Phys. Radium **22**, 329 (1961).
[19] B. S. Mathur, H. Tang, and W. Happer, Phys. Rev. **171**, 11 (1968).
[20] S. Appelt, A. B.-A. Baranga, A. R. Young, and W. Happer, Phys. Rev. A **59**, 2078 (1999).
[21] J. Vanier, J.-F. Simard, and J.-S. Boulanger, Phys. Rev. A **9**, 1031 (1974).
[22] J. Vanier (private communication).
[23] W. E. Bell and A. L. Bloom, Phys. Rev. Lett. **6**, 280 (1961).
[24] G. Alzetta, A. Gozzini, L. Moi, and G. Orriois, Nuovo Cimento Soc. Ital. Fis. B **36B**, 5 (1976).